



CHORUS

This is the accepted manuscript made available via CHORUS. The article has been published as:

Dilution and resonance-enhanced repulsion in nonequilibrium fluctuation forces

Giuseppe Bimonte, Thorsten Emig, Matthias Krüger, and Mehran Kardar

Phys. Rev. A **84**, 042503 — Published 5 October 2011

DOI: [10.1103/PhysRevA.84.042503](https://doi.org/10.1103/PhysRevA.84.042503)

Dilution and resonance enhanced repulsion in non-equilibrium fluctuation forces

Giuseppe Bimonte,^{1,2} Thorsten Emig,³ Matthias Krüger,⁴ and Mehran Kardar⁴

¹*Dipartimento di Scienze Fisiche, Università di Napoli Federico II,
Complesso Universitario MSA, Via Cintia, I-80126 Napoli, Italy*

²*INFN Sezione di Napoli, I-80126 Napoli, Italy*

³*Laboratoire de Physique Théorique et Modèles Statistiques,
CNRS UMR 8626, Bât. 100, Université Paris-Sud, 91405 Orsay cedex, France*

⁴*Massachusetts Institute of Technology, Department of Physics, Cambridge, Massachusetts 02139, USA*

In equilibrium, forces induced by fluctuations of the electromagnetic field between electrically polarizable objects (microscopic *or* macroscopic) in vacuum are generically attractive. The force may, however, become repulsive for microscopic particles coupled to thermal baths with different temperatures. We demonstrate that this non-equilibrium repulsion can be realized also between macroscopic objects, as planar slabs, if they are kept at different temperatures. It is shown that repulsion can be enhanced by (i) tuning of material resonances in the thermal region, and by (ii) reducing the dielectric contrast due to “dilution”. This can lead to stable equilibrium positions. We discuss the realization of these effects for aerogels, yielding repulsion down to sub-micron distances at realistic porosities.

PACS numbers: 12.20.-m, 44.40.+a, 05.70.Ln

Forces induced by electromagnetic (EM) field fluctuations of quantum and thermal origin act virtually between all matter that couples to the EM field, since the interacting objects need not to be charged [1, 2]. Under rather general conditions (e. g., for non-magnetic objects in vacuum), the Casimir potential energy does not allow for stable equilibrium positions of the interacting objects [4]. This can be a practical disadvantage in systems where external (non-fluctuation) forces cannot be applied or fine-tuned to establish stability, especially in dynamic systems where the distance and hence the Casimir force changes in time. Nano-mechanical devices with closely spaced components fall into this class of systems [5]. Repulsive Casimir forces are known to exist if the space between the objects is filled by a dielectric with suitable contrast [3], but this is impractical in many situations.

Repulsion can occur also in response to the preparation of particles in distinct internal states, e.g. by optical excitation or coupling to heat baths of different temperatures. In particular, Cohen and Mukamel [6] predicted a non-equilibrium repulsive force between molecules generated by suitable detuning of the resonance frequencies. This suggests that for macroscopic objects held at different temperatures similar repulsive effects should exist close to material resonances in the thermal region. However, for macroscopic condensates the dielectric contrast is usually strong and non-equilibrium effects are comparatively less significant than the equilibrium attraction. One should thus focus on sufficiently optically diluted materials to generate resonant Casimir repulsive forces between macroscopic bodies. The general formalism for dealing with non-equilibrium fluctuation effects between macroscopic bodies has been developed recently in [7–11].

The aim of the present work is to explore theoretically if and to what extent the above expectation can be realized and whether it can lead to stable equilibrium positions. We consider two dielectric slabs held at dif-

ferent temperatures, and computed the pressure between them using the non-equilibrium extension of the Casimir–Lifshitz formula [7]. Employing a Lorentz-Drude dielectric response, we find that resonances and optical dilution indeed amplify repulsion sufficiently so that the total interaction can become repulsive, and equilibrium positions exist. We show that aerogels could be used to realize resonant repulsion in practice since porosity can be used to tune reflectivity and resonances. The use of aerogels was indeed previously proposed to reduce the Casimir force [12], but not to generate repulsion.

We consider two infinite parallel planar slabs \mathcal{S}^α , $\alpha = 1, 2$, each consisting of a non-magnetic dielectric layer of thickness δ and permittivity $\epsilon_\alpha(\omega)$, deposited on a thick glass substrate of dielectric permittivity $\epsilon_{\text{sub}}(\omega)$. The slabs are held at temperatures T_1 and T_2 , separated by a (vacuum) gap of width a . The Casimir pressure [18] acting on the inside faces of the plates is given by [7]

$$P_{\text{neq}}(T_1, T_2, a) = \bar{P}_{\text{eq}}(T_1, T_2, a) + \Delta P_{\text{neq}}(T_1, T_2, a) + \frac{2\sigma}{3c}(T_1^4 + T_2^4), \quad (1)$$

where σ is the Stefan-Boltzmann constant. The last term in this equation is simply the classical thermal radiation result, which is independent of distance and material properties. In Eq. (1), $\bar{P}_{\text{eq}}(T_1, T_2, a) = [P_{\text{eq}}(T_1, a) + P_{\text{eq}}(T_2, a)]/2$ denotes the average of the equilibrium Casimir pressures at T_1 and T_2 ; with $P_{\text{eq}}(T, a)$ given by the Lifshitz formula [14], which for brevity is not reproduced here. The novel non-equilibrium contributions are captured by the term $\Delta P_{\text{neq}}(T_1, T_2, a)$, which vanishes for $T_1 = T_2$ (it also contains a distance independent part). Upon decomposing $\Delta P_{\text{neq}} = \Delta P_{\text{neq}}^{\text{PW}} + \Delta P_{\text{neq}}^{\text{EW}}$ into propagating waves (PW) and evanescent waves (EW), one

finds

$$\begin{aligned} \Delta P_{\text{neq}}^{\text{PW}} &= \frac{\hbar}{4\pi^2} \sum_{P=M,N} \int_0^\infty d\omega [n(T_1) - n(T_2)] \\ &\times \int_0^{\omega/c} dk_\perp k_\perp k_z \frac{|r_P^{(2)}|^2 - |r_P^{(1)}|^2}{|D_P|^2}, \quad (2) \\ \Delta P_{\text{neq}}^{\text{EW}} &= -\frac{\hbar}{2\pi^2} \sum_{P=M,N} \int_0^\infty d\omega [n(T_1) - n(T_2)] \int_{\omega/c}^\infty dk_\perp k_\perp \\ &\times \text{Im}(k_z) e^{-2a\text{Im}(k_z)} \frac{\text{Im}(r_P^{(1)})\text{Re}(r_P^{(2)}) - \text{Re}(r_P^{(1)})\text{Im}(r_P^{(2)})}{|D_P|^2}, \quad (3) \end{aligned}$$

where $n(T) = [\exp(\hbar\omega/k_B T) - 1]^{-1}$, $k_z = \sqrt{\omega^2/c^2 - k_\perp^2}$, $D_P = 1 - r_P^{(1)} r_P^{(2)} \exp(2ik_z a)$, and $P = M, N$ for the two polarizations. The reflection coefficients $r_P^{(\alpha)}(\omega, k_\perp)$ are given by the well-known formulae for a two-layer slab

$$r_P^{(\alpha)} = \frac{r_P(1, \epsilon_\alpha) + r_P(\epsilon_\alpha, \epsilon_{\text{sub}}) e^{2i\delta q_\alpha}}{1 + r_P(1, \epsilon_\alpha) r_P(\epsilon_\alpha, \epsilon_{\text{sub}}) e^{2i\delta q_\alpha}}, \quad (4)$$

where $r_P(\epsilon_a, \epsilon_b)$ are the Fresnel reflection coefficients

$$r_N(\epsilon_a, \epsilon_b) = \frac{\epsilon_b(\omega) q_a(\omega, k_\perp) - \epsilon_a(\omega) q_b(\omega, k_\perp)}{\epsilon_a(\omega) q_b(\omega, k_\perp) + \epsilon_b(\omega) q_a(\omega, k_\perp)}, \quad (5)$$

where $q_a = \sqrt{\epsilon_a(\omega)\omega^2/c^2 - k_\perp^2}$, and $r_M(\epsilon_a, \epsilon_b)$ is obtained by replacing the ϵ_a and ϵ_b in Eq. (5) by one (but not in q_a). There is also an external pressure acting on the outside face of each plate which depends on the reflectivity of this face and the temperature of the environment T_{env} . In our numerical computations we assume that the external face of the glass substrate has been blackened, in which case the total pressure on plate α is given by

$$\tilde{P}^{(\alpha)}(T_1, T_2, T_{\text{env}}, a) = P_{\text{neq}}(T_1, T_2, a) - \frac{2\sigma}{3c}(T_\alpha^4 + T_{\text{env}}^4). \quad (6)$$

It is worth emphasizing that for $T_1 \neq T_2$, $\tilde{P}^{(1)}(T_1, T_2, T_{\text{env}}, a) \neq \tilde{P}^{(2)}(T_1, T_2, T_{\text{env}}, a)$. Also, in equilibrium all distance independent terms vanish.

The structure of the non-equilibrium force in Eq. (1) suggests that repulsion should exist out of thermal equilibrium. While the first term $\bar{P}_{\text{eq}}(T_1, T_2, a)$ in Eq. (1) is bound to be attractive, this is not so for the second term $\Delta P_{\text{neq}}(T_1, T_2, a)$. As it can be seen from Eqs. (2) and (3), the quantity $\Delta P_{\text{neq}}(T_1, T_2, a)$ changes sign if the temperatures T_1 and T_2 are exchanged, and therefore its sign can be reversed by simply switching the temperatures of the plates. One notes also that $\Delta P_{\text{neq}}(T_1, T_2, a)$ is *antisymmetric* under the exchange $r_P^{(1)} \leftrightarrow r_P^{(2)}$, and vanishes for $r_P^{(1)} = r_P^{(2)}$. Therefore in order to take advantage of this term to control the sign of the Casimir force it is mandatory to consider plates made of *different* materials. For real materials, both $\bar{P}_{\text{eq}}(T_1, T_2, a)$ and $\Delta P_{\text{neq}}(T_1, T_2, a)$ diverge as a^{-3} if $a \rightarrow 0$. In the following, we show that the sign of this asymptotic behavior can be made repulsive in certain cases.

Motivated by the resonance-induced repulsion for microscopic particles, we consider electric permittivities $\epsilon_\alpha(\omega)$ of the dielectric layers described by a Lorentz-Drude type model, as

$$\epsilon_\alpha(\omega) = 1 + \frac{C_\alpha \omega_\alpha^2}{\omega_\alpha^2 - \omega^2 - i\gamma_\alpha \omega} + \frac{D_\alpha \Omega_\alpha^2}{\Omega_\alpha^2 - \omega^2 - i\Gamma_\alpha \omega}. \quad (7)$$

(An analogous two-oscillator model was used also for the permittivity ϵ_{sub} of the glass substrate, with the parameters quoted in [2], p. 312.) The first oscillator term ($\sim C_\alpha$) describes low-lying excitations of the materials; such low-lying polariton excitations in numerous dielectrics account for sharp peaks in their dielectric functions in the far infrared region. Typical values for the resonance and relaxation frequencies are $\omega_\alpha = 10^{13} - 10^{14}$ rad/sec and $\gamma_\alpha = 10^{11} - 10^{12}$ rad/sec [15]. The second oscillator term in Eq. (7), proportional to D_α , describes the contribution of core electrons. Excitation energies of core electrons are much larger, and characteristic values of Ω_α are in the range $10^{15} - 10^{16}$ rad/sec. At and around room temperature core electrons are not thermally excited (for $T = 300\text{K}$ the characteristic thermal frequency $\omega_T = k_B T/\hbar$ is 3.9×10^{13} rad/sec) and therefore their contribution to the thermal Casimir force ΔP_{neq} is very small. However core electrons are important, as they strongly contribute to the average equilibrium Casimir force \bar{P}_{eq} , especially at sub-micron separations.

Since the thermal Casimir force between two macroscopic slabs should reduce in the dilute limit to the pairwise interaction between their atoms, one expects that the resonant phenomena reported in Ref. [6] should be recovered if the material of the plates is sufficiently diluted. In order to determine how large a dilution is necessary for this to happen, we investigated the behavior of the Casimir force under a rescaling of the amplitudes of the resonance peaks, i.e. $C_\alpha \rightarrow C_\alpha/\tau$, $D_\alpha \rightarrow D_\alpha/\tau$ by a overall optical dilution parameter $\tau \geq 1$.

We next report on numerical results based upon the above model for dielectrics, in which we set $\omega_1 = 10^{13}$, $\gamma_1 = \gamma_2 = 10^{11}$, $\Omega_1 = \Omega_2 = 10^{16}$, and $\Gamma_1 = \Gamma_2 = 5 \times 10^{14}$ (all in rad/sec). In Fig. 1 we plot the non-equilibrium normalized Casimir pressure $P_{\text{neq}}^{(2)}/\bar{P}_{\text{eq}}$ on slab 2 versus the ratio of the resonance frequencies ω_2/ω_1 , for $a = 300$ nm, $\delta = 5 \mu\text{m}$, $C_1 = 3$, $C_2 = 1.5$, $D_1 = 1$, and $D_2 = 0.5$. (Negative values of $P_{\text{neq}}^{(2)}/\bar{P}_{\text{eq}}$ correspond to repulsion.) For these parameters the non-equilibrium force is dominated by evanescent waves, whose skin depth is comparable to the separation a . This implies that for separations $a \ll \delta$ the force is practically independent of δ , but for $a \gtrsim \delta$ the features of the substrate influence the magnitude of the force significantly. The red dashed curves in Fig. 1 are for $T_1 = T_{\text{env}} = 300\text{K}$ and $T_2 = 600\text{K}$, while blue solid curves are for $T_1 = T_{\text{env}} = 300\text{K}$ and $T_2 = 150\text{K}$. Three values of the dilution parameter τ are displayed: $\tau = 1$ (\times), $\tau = 10$ ($+$) and $\tau = 20$ ($*$). We see that for sufficiently high dilution, the Casimir force is strongly dependent on the ratio ω_2/ω_1 of the resonance

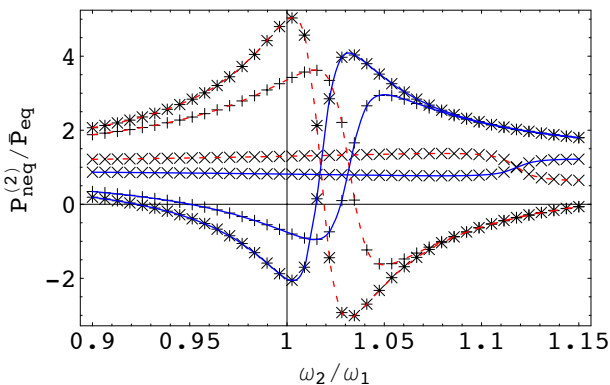


FIG. 1: (Color online) The normalized non-equilibrium Casimir pressure $P_{\text{neq}}^{(2)}/\bar{P}_{\text{eq}}$ on slab 2 as a function of the ratio of the resonance frequencies ω_2/ω_1 , for $a = 300$ nm, $\delta = 5$ μm , $C_1 = 3$, $C_2 = 1.5$, $D_1 = 1$, and $D_2 = 0.5$. The red dashed curves are for $T_1 = T_{\text{env}} = 300\text{K}$ and $T_2 = 600\text{K}$, while blue solid curves are for $T_1 = T_{\text{env}} = 300\text{K}$ and $T_2 = 150\text{K}$. Three values of the dilution parameter τ are displayed: $\tau = 1$ (\times), $\tau = 10$ ($+$) and $\tau = 20$ ($*$). Negative values of $P_{\text{neq}}^{(2)}/\bar{P}_{\text{eq}}$ correspond to repulsion.

frequencies of the plates, displaying features analogous to those reported in Ref. [6] for the van der Waals interaction between two ‘atoms’ coupled to baths at different temperatures. In particular, the Casimir force becomes repulsive if this ratio is suitably tuned to a value close to unity. We also find that the equilibrium force is rather insensitive to the tuning of resonances, and that the total force hardly depends on Ω_1/Ω_2 .

In Fig. 2 we plot the dependence of the non-equilibrium normalized Casimir pressure $P_{\text{neq}}^{(2)}/\bar{P}_{\text{eq}}$ on slab 2, as a function of plate separation a , at $T_1 = T_{\text{env}} = 300\text{K}$, $T_2 = 600\text{K}$, for $\tau = 1$ and $\omega_2/\omega_1 = 1.1$ (\times); $\tau = 10$ and $\omega_2/\omega_1 = 1.05$ ($+$); $\tau = 20$ and $\omega_2/\omega_1 = 1.04$ ($*$), all other parameters being same as in Fig. 1. The dashed curves do not include the distance independent part of the pressure, and are included to indicate that this component also changes sign upon dilution. We see that without dilution ($\tau = 1$) the non-equilibrium Casimir force is attractive for all displayed separations. By contrast, for large enough dilutions and for suitable values of ω_2/ω_1 , the force becomes repulsive in a wide range of separations. The curve for $\tau = 10$ exhibits two points of zero force, one at $a = 15$ nm and another for $a = 4.1$ μm , corresponding to an unstable equilibrium point (UEP) and a stable equilibrium point (SEP), respectively. For $\tau = 20$ there is a single turning point corresponding to a SEP at $a = 3.3$ μm . There is no UEP point in this case as the ratio $P_{\text{neq}}^{(2)}/\bar{P}_{\text{eq}}$ approaches a negative value in the limit $a \rightarrow 0$, signifying that repulsion persists for arbitrarily small plate separations less than the SEP.

As a means of achieving the dilution levels required to observe the resonance phenomena described above, we consider aerogels: highly porous materials fabricated by sol-gel techniques, starting from a variety of materials

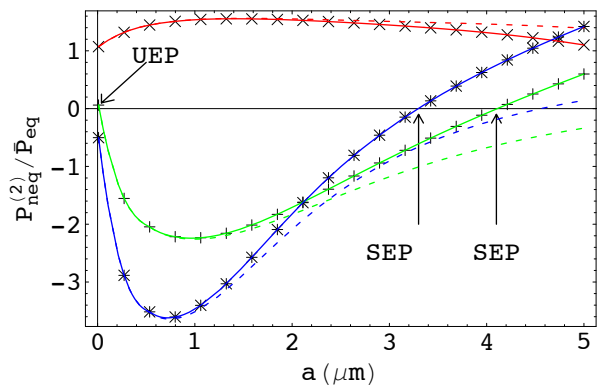


FIG. 2: (Color online) The non-equilibrium normalized Casimir pressure $P_{\text{neq}}^{(2)}/\bar{P}_{\text{eq}}$ on slab 2 as a function of plate separation (in microns) for $\delta = 5$ μm , $T_1 = T_{\text{env}} = 300\text{K}$, $T_2 = 600\text{K}$, $\tau = 1$ and $\omega_2/\omega_1 = 1.1$ (\times), $\tau = 10$ and $\omega_2/\omega_1 = 1.05$ ($+$), for $\tau = 20$ and $\omega_2/\omega_1 = 1.03$ ($*$). All other parameters are same as in Fig. 1. Dashed curves do not include the distance independent part of the pressure. Stable equilibrium positions are marked as SEP, unstable ones as UEP. The curve for $\tau = 20$ approaches a negative values $a \rightarrow 0$.

such as SiO_2 , carbon, Al_2O_3 , platinum etc. Aerogels with levels of porosity exceeding 99% can be realized nowadays [16]. In order to study the Casimir force between two aerogel plates we need an expression for the dielectric function $\hat{\epsilon}(\omega)$ of the aerogel, valid in the wide range of frequencies relevant for the Casimir effect. For separations a larger than the pore size (typically of the order of 100 nm or less), an effective medium approach can be used in which the aerogel permittivity $\hat{\epsilon}(\omega)$ is obtained from the Maxwell-Garnett equation [17] as

$$\frac{\hat{\epsilon} - 1}{\hat{\epsilon} + 2} = (1 - \phi) \frac{\epsilon - 1}{\epsilon + 2}. \quad (8)$$

Here, $\epsilon(\omega)$ is the permittivity of the solid fraction of the aerogel, and $0 \leq \phi \leq 1$ is the porosity. Equation (8) is justified if the solid fraction is well separated by the host material (air), i.e., when ϕ is sufficiently close to one. Using again a model of the form in Eq. (7) for $\epsilon_\alpha(\omega)$, one finds that $\hat{\epsilon}_\alpha(\omega)$ has a resonance at the frequency

$$\hat{\omega}_\alpha \approx \left(1 + \frac{\phi_\alpha C_\alpha}{\phi_\alpha D_\alpha + 3}\right)^{1/2} \omega_\alpha, \quad (9)$$

where we assumed $\omega_\alpha \ll \Omega_\alpha$. According to Eq. (9), the frequency of the aerogel resonance is blue-shifted with respect to ω_α , and as ϕ_α is varied from zero to one, $\hat{\omega}_\alpha$ sweeps the range from ω_α to $[1 + C_\alpha/(D_\alpha + 3)]^{1/2} \omega_\alpha$. The dependence of the resonance frequency $\hat{\omega}_\alpha$ on the porosity is welcome, because it gives us the possibility of tuning the ratio of the resonance frequencies for the two plates by simply choosing appropriate values for the porosities ϕ_1 and ϕ_2 of the plates.

As an example, we consider two aerogel layers of thickness $\delta = 5$ μm , deposited on a thick glass substrate, with a

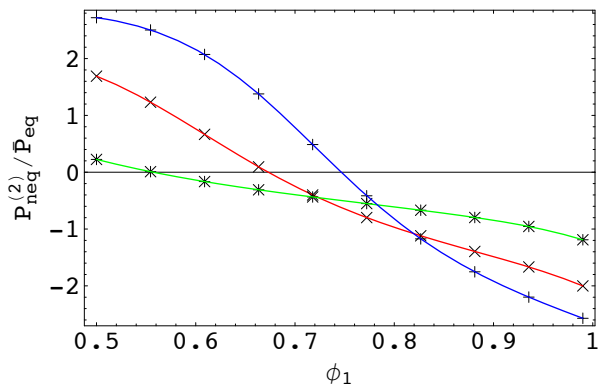


FIG. 3: (Color online) The pressure ratio $P_{\text{neq}}^{(2)}/\bar{P}_{\text{eq}}$ for two aerogel layers ($\delta = 5 \mu\text{m}$) on a glass substrate as a function of the porosity ϕ_1 of plate one. The porosity ϕ_2 of plate two is 0.95 (+), 0.9 (x) and 0.8 (*). The dielectric functions $\epsilon_\alpha(\omega)$ of the host materials are as in Eq. (7), with $C_1 = 1$, $C_2 = 3$, $D_1 = D_2 = 0.5$, $\omega_2/\omega_1=0.84$. All curves are for a separation of 200 nm and for $T_1 = T_{\text{env}} = 300 \text{ K}$, $T_2 = 600 \text{ K}$.

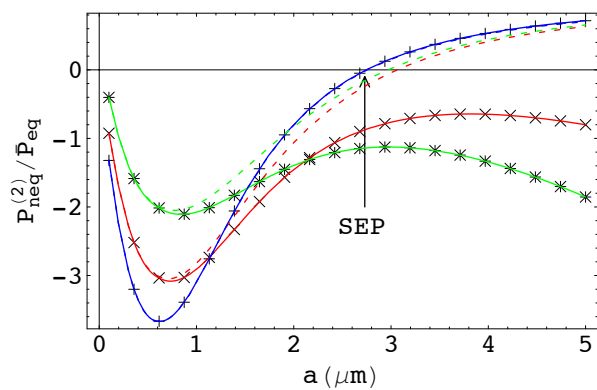


FIG. 4: (Color online) The pressure ratio $P_{\text{neq}}^{(2)}/\bar{P}_{\text{eq}}$ for two aerogel layers ($\delta = 5 \mu\text{m}$) on a glass substrate as a function of plate separation (in microns), for $\phi_1 = 0.95$ and $\phi_2=0.95$ (+), 0.9 (x) and 0.8 (*). All parameters for the aerogel plates are same as in Fig. 3. The dashed lines do not include the separation independent part of the pressure. The stable equilibrium position is marked by SEP.

blackened outer surface. The dielectric functions $\epsilon_\alpha(\omega)$ of the host materials are as in Eq. (7), with $C_1 = 1$, $C_2 = 3$, $D_1 = D_2 = 0.5$, $\omega_2/\omega_1=0.84$. In Fig. 3 we plot the ratio $P_{\text{neq}}^{(2)}/\bar{P}_{\text{eq}}$ as a function of the porosity ϕ_1 of the first plate. The porosity ϕ_2 of the second plate is 0.95 (+), 0.9 (x) and 0.8 (*). All curves in Fig. 3 are for a separation of 200 nm, at $T_1 = T_{\text{env}} = 300 \text{ K}$ and $T_2 = 600 \text{ K}$. The force can indeed be made repulsive by suitably adjusting the porosities of the two plates. In absolute terms, the Casimir force is small; e.g. for $\phi_1 = 0.77$ and $\phi_2 = 0.8$ we find $P_{\text{neq}}^{(2)} = 0.55 \times 10^{-3} \text{ Pa}$.

In Fig. 4 we plot dependence of the ratio $P_{\text{neq}}^{(2)}/\bar{P}_{\text{eq}}$ on the separation (in microns), for $\phi_1 = 0.95$ and $\phi_2=0.95$ (+), $\phi_2=0.9$ (x) and $\phi_2=0.8$ (*). All parameters for the aerogel plates are the same as in Fig. 3. The dashed lines do not include the separation independent part of the pressure. We find that for $\phi_1 = \phi_2 = 0.95$ a stable equilibrium point exists (marked as SEP in Fig. 4).

While fluctuation induced forces are generally attractive, repulsive forces can be obtained between atoms prepared in different excited states. Coupling of atoms to thermal baths at different temperatures can in principle produce population of states that lead to repulsion. We show that a similar non-equilibrium repulsive contribution to pressure also arises from the interplay of resonances for two macroscopic slabs held at appropriate distinct temperatures. However, to observe a net repulsion between slabs one must overcome an ever present attractive force arising from the dielectric contrast of the condensed bodies from the intervening vacuum. The latter can be reduced by dilution, and we have shown that aerogels provide a material where a net repulsion at sub-micron separations can be achieved, leading to a stable equilibrium point.

This research was supported by the ESF Research Network CASIMIR, DARPA contract No. S-000354, DFG grant No. KR 3844/1-1 and NSF Grant No. DMR-08-03315. We have benefitted from discussions with R.L. Jaffe, M.F. Maghrebi, U. Mohideen, and R. Zandi.

-
- [1] V. A. Parsegian, *Van der Waals Forces* (Cambridge University Press, 2006).
 - [2] M. Bordag, G. L.Klimchitskaya, U. Mohideen, and V. M. Mostepanenko, *Advances in the Casimir Effect* (Oxford University Press, Oxford, 2009).
 - [3] I. E. Dzyaloshinskii, E. M. Lifshitz, L. P. Pitaevskii, *Adv. Phys.* **10**, 165 (1961).
 - [4] S. J. Rahi, M. Kardar, T. Emig, *Phys. Rev. Lett.* **105**, 070404 (2010).
 - [5] F. M. Serry, D. Walliser, and G. J. Maclay, *J. Microelectromech. Syst.* **4**, 193 (1995); *J. Appl. Phys.* **84**, 2501 (1998).
 - [6] A.E. Cohen and S. Mukamel, *Phys. Rev. Lett.* **91**, 233202 (2003).
 - [7] M. Antezza, L.P. Pitaevskii, S. Stringari and V.B. Svetovoy, *Phys. Rev A* **77**, 022901 (2008).
 - [8] G. Bimonte, *Phys. Rev. A* **80**, 042102 (2009).
 - [9] M. Krüger, T. Emig, M. Kardar, *Phys. Rev. Lett.* **106**, 210404 (2011).
 - [10] R. Messina and M. Antezza, arXiv:1103.2668.
 - [11] M. Krüger, T. Emig, G. Bimonte, and M. Kardar, *Europhys. Lett.* **95**, 21002 (2011).
 - [12] R. Esquivel-Sirvent, *J. Appl. Phys.* **102**, 034307 (2007).
 - [13] C. Henkel, K. Joulain, J-P Mulet, and J-J Greffet, *J. Opt.A: Pure Appl. Opt.* **4**, S109 (2002).
 - [14] E.M. Lifshitz, *Sov. Phys. JETP* **2**, 73 (1956); E.M. Lifshitz and L.P. Pitaevskii, *Landau and Lifshitz Course of Theoretical Physics: Statistical Physics Part II*

- (Butterworth-Heinemann, 1980)
- [15] C. Kittel, *Introduction to Solid State Physics* (Wiley, 2005), p. 416.
- [16] A. C. Pierre, and G. M. Pajonk, *Chem. Rev.* **102**, 4243 (2002).
- [17] T. C. Choy, *Effective Medium Theory* (Oxford: Clarendon Press, 1999), p. 7.
- [18] We use a sign convention opposite to Ref. [7], such that negative pressures represent attraction between the slabs.